Journal of Materials Chemistry B

PAPER

View Article Online
View Journal | View Issue

Cite this: J. Mater. Chem. B, 2014, 2, 1838

Synthesis and antibacterial properties of a hybrid of silver–potato starch nanocapsules by miniemulsion/polyaddition polymerization

Shima Taheri,[a] Grit Baier,[b] Peter Majewski,[a] Mary Barton,[c] Renate Förch,[b] Katharina Landfester*[b] and Krasimir Vasilev*[ad]

Received 29th November 2013
Accepted 9th January 2014

DOI: 10.1039/c3tb21690j

www.rsc.org/MaterialsB

Controlled synthesis of hollow polymeric nanocapsules has attracted significant attention in a wide range of applications. This paper reports a facile method for the synthesis of hybrid starch nanocapsules decorated with silver nanoparticles using the inverse miniemulsion polyaddition technique. Silver nanoparticles are formed and embedded in the shell of the nanocapsules during the polyaddition process without using any additional reducing agents. We found that silver also acts as a lipophobe that builds up osmotic pressure in the droplets facilitating the formation of stable round shaped nanocapsules. The nanocapsules' shell thickness could be tuned from 13 to 29 nm by varying the amount of cross-linker. We investigated the minimum inhibitory concentration (MIC) of the nanocapsules against *Staphylococcus epidermidis* ATCC 35984 and *Escherichia coli* ATCC 25922 which are two bacteria of medical relevance. The silver nanoparticle decorated nanocapsules showed antibacterial properties against both bacteria at the MIC of 2.315 μg mL^{-1} while control nanocapsules without silver had no antibacterial activity.

1. Introduction

Infections are the second leading cause of death worldwide after heart diseases. The importance of the problem has led to extensive prevention and treatment efforts. However, despite great examples of success, infections are still part of our society causing suffering, death and substantial burden to the healthcare systems.[1,2] Today, the main weapons to fight infections are antibiotics. This therapy saved millions of lives over the last 60 years; however, it has some disadvantages.[3] One of the major problems is the phenomenon associated with antimicrobial resistance.[4,5] Since the 1970s, a trend to returning to silver and silver based compounds after the development of antibiotic resistance has emerged.[6,7] Over the last two decades, there has been increased interest in the use of silver, silver compounds and silver nanoparticles in medical applications. Examples are coatings for applications on wound dressing[8,9] and medical devices such as catheters.[10,11] A number of commercial silver and silver nanoparticle containing products are currently on the market. A vast number of research papers on the subject have also been published. For further reading, we direct the reader to several recent reviews on the topic.[12–19] The reasons for this trend are that silver is universally active against all bacteria and not limited to certain bacterial types as antibiotics. Importantly, there is no convincing evidence that medically relevant bacteria are capable of developing resistance to silver.[20,21]

The goal of this work is to generate advanced biocompatible nanocapsules which are decorated with silver nanoparticles. Nanocapsules have been shown to be promising carries of drugs and other therapeutic molecules.[22] The underlying motivation is to add antibacterial properties to nanocapsules' transport capability. We selected miniemulsion polymerization to achieve our goal. The technique is facile and provides molecular control over nanocapsule dimensions, structure and chemical composition.[22] Narrowly distributed small droplets resulting from this process can act as nano-carriers or nano-reactors which makes them attractive in many applications such as targeted drug delivery systems,[23,24] self-healing coatings,[25–27] and optical molecular imaging.[28] The technique has already been demonstrated for the successful encapsulation of a variety of materials such as nanoparticles, pigments, polymers, fragrances, drugs, and photoinitiators.[22,29] We chose potato starch as the organic component for generating the nanocapsule wall structure because of its biocompatible and biodegradable nature.[30] Starch nanocapsules have already been demonstrated as drug carriers

[a]School of Engineering, University of South Australia, Mawson Lakes, SA 5095, Australia. E-mail: krasimir.vasilev@unisa.edu.au; Fax: +61 8 83025689; Tel: +61 8 83025697

[b]Max Planck Institute for Polymer Research, Ackermannweg 10, 55128 Mainz, Germany. E-mail: landfester@mpip-mainz.mpg.de; Fax: +49 6131 379 370; Tel: +49 6131 379 170

[c]School of Pharmacy and Medical Sciences, University of South Australia, SA 5000, Australia

[d]Mawson Institute, University of South Australia, Mawson Lakes, SA 5095, Australia

with potential in targeted drug delivery and therapies.[31,32] This study further aims to demonstrate the capacity to control the capsule wall thickness. In addition, we aim to provide functional chemical groups of the outer wall of the capsules which can be used for attachment of ligands for different applications (*i.e.* antibodies for cell targeting) or immobilization to surfaces.

2. Experimental

2.1. Materials

All reagents were used as received without further purification. The hydrophilic water-soluble potato starch MW 15 000 g mol^{-1} (determined by GPC-MALLS) was purchased from Fluka. Silver nitrate ($AgNO_3$, 99.99%), 2,4-toluene diisocyanate (TDI) and cyclohexane (>99.9%) were purchased from Sigma Aldrich. The oil soluble surfactant polyglycerin-polyricinoleat (PGPR) was purchased from Danisco (GRINDSTED®PGPR). The non-ionic surfactant Lutensol AT50, which is a poly(ethylene oxide)-hexadecyl ether with an EO block length of about 50 units, was provided by BASF. Sterilized water aqua ad iniectabilia was obtained from Braun. Monochloroacetic acid (MCA) was purchased from Aldrich.

2.2. Instrumental

A PSS Nicomp Particle Sizer 380 (Nicomp Particle Sizing Systems, USA) was used to measure the average size and size distribution of the nanocapsules. High resolution scanning electron microscopy (SEM) (Hitachi S-5200) and Transmission Electron Microscopy (TEM) (Philips CM200) were carried out to determine the particles' morphology. Samples were prepared by drying a droplet of diluted samples on silicon wafer for SEM and carbon coated copper grids for TEM. FTIR measurements were carried out using a Perkin Elmer Spectrum BX in the spectral range between 4000 and 400 cm^{-1} to determine the chemical composition of the nanocapsules. The equipment used for measuring the particle charge of nanocapsules was PCD 02 (Mütek Company) equipped with a Mettler DL21 Titrator. The amount of silver present in nanocapsules was analyzed by inductively coupled plasma (ICP) spectroscopy using a Perkin Elmer ICP-OES Optima 7300 DV to analyze Ag (mg L^{-1}). The reading wavelength for Ag was 328.068 nm and the collected data were processed with MSF (Multicomponent Spectral Fitting).

2.3. Solid content measurement

The solid content of each sample was measured gravimetrically. An empty scintillation vial was weighed and the weight was recorded to the nearest thousandth of a gram (A). 100 μL of sample was then added to the vial and the weight was recorded (B). The specimen was then placed in an oven with temperature set at 105 °C for 3 hours. The dried specimen was then removed from the oven and the weight was recorded to the nearest thousandth of a gram (C). The following equation calculates the percent of solids

$$\%\text{Total solid (solid content)} : \frac{\left[\begin{array}{l}\text{weight of dried sample plus dish } (C) - \\ \text{weight of empty dish } (A)\end{array}\right]}{\left[\begin{array}{l}\text{weight of original sample plus dish } (B) \\ -\text{weight of empty dish } (A)\end{array}\right]} \times 100 \quad (1)$$

2.4. Synthesis of starch–silver nanocapsules

First, an aqueous solution consisting of 0.057 g $AgNO_3$, 1.300 g sterilized water and 0.100 g soluble potato starch was prepared. To this phase, 7.400 g of cyclohexane pre-mixed with 0.100 g PGPR was added and stirred at 1000 rpm for one hour at 25 °C using a magnetic stirrer. Then the mixture was ultrasonicated for 180 s at 90% amplitude in a pulse regime (20 s sonication, 10 s pause) using a Branson Sonifier W-450-Digital and a 1/2″ tip under ice cooling conditions in order to prevent evaporation of the solvent. Different amounts (0.200, 0.150 and 0.100 mg) of TDI dissolved in 4.970 g of cyclohexane and pre-mixed with 0.030 g PGPR were added dropwise over 5 min to the previously prepared emulsion under stirring conditions while maintaining the temperature at 25 °C. The mixture was kept under stirring overnight at 25 °C. The miniemulsion samples were then dispersed in 0.3% Lutensol AT50 at a ratio of 1 : 5. Another set of samples was prepared according to the procedure described above but without $AgNO_3$. The designation and formulation compositions used in this study are denoted in Table 1.

2.5. Carboxymethylation of starch–silver nanocapsules

The carboxymethylation of starch–AgNP nanocapsules was performed using a method published previously.[24] Briefly, 0.4 mL of NaOH solution (0.1 M) was added to 4.0 g of starch–AgNP re-dispersion nanocapsules (solid content 1.0 wt%) and stirred at ambient temperature for 24 h to neutralize the non-reacted hydroxyl groups of the starch molecules on the nanocapsule surface. Next, 40 μL of MCA (20.0 wt%) was mixed with the above mentioned dispersion and stirred for 24 h at 40 °C. Then 0.2 mL of NaOH solution (1.0 M) was added to the solution and stirred again for 24 h at ambient temperature. Finally, the nanocapsule dispersion was centrifuged at 4000 rpm for 20 min (Sigma 3k-30, RCF 1467) and after removing the supernatant starch–AgNP nanocapsules were redispersed in demineralized water. The amount of carboxylic groups was determined by the

Table 1 Formulations used in the synthesis of nanocapsules

	Chemistry			
Sample name	$AgNO_3$ (mg)	H_2O (g)	Starch (mg)	TDI (mg)
S043	57	1.3	100	200
S044	57	1.3	100	150
S045	57	1.3	100	100
S046	0	1.3	100	200
S047	0	1.3	100	150
S048	0	1.3	100	100

polyelectrolyte titration method described below. Carboxyl acid groups were titrated against poly-DADMAC using 10 mL of the dispersion with a solid content of 0.01 g L^{-1} at a pH of 10. Each sample was titrated in triplicate, the number of carboxyl acid groups per nm^2 was determined from the average consumed volume of the titrant using the following equations:[33]

$$\left[\text{groups per } g_{\text{polymer}}\right] = \frac{VMN_A}{SC} \text{ (the quantity of charged groups per nm}^2\text{)} \quad (2)$$

$$\left[\text{groups per particle}\right] = \left[\text{groups per } g_{\text{polymer}}\right] \frac{\rho {D_n}^3 \pi}{SC} \text{ (the quantity of charged groups per particle)} \quad (3)$$

$$\left[\text{groups per nm}^2\right] = \left[\text{groups per } g_{\text{polymer}}\right] \frac{\rho D_n 10^{-18}}{6} \text{ (the quantity of charged groups per square unit)} \quad (4)$$

V = volume of the consumed polyelectrolyte in liters, M = molar concentration of the polyelectrolyte in moles per liter, F = density of polystyrene (1.045×10^6 g L^{-1}), N_A = Avogadro's constant, SC = solid content of the sample in grams, D_n = average number diameter of the particle.

2.6. Determination of antibacterial activity *in vitro*

Staphylococcus epidermidis (ATCC 35984) and *Escherichia coli* (ATCC 25922) were used because these are common microorganisms involved in hospital-acquired infections. The nanocapsules were assayed for activity against these two strains *in vitro*.[34] Bacteria were plated on Luria–Bertani agar plates from frozen stocks and incubated at 37 °C. Individual bacterial colonies were picked and incubated overnight at 37 °C in the oven. Nanocapsules were washed and serially diluted in quadruplicate in a 96 well microtiter plate with a final volume of 50 μL per well. ABS_{600} was used to adjust to approximately 1×10^8 CFU mL^{-1} and further diluted to 1.33×10^6 CFU mL^{-1} in tryptic soya broth (TSB). A total of 150 μL of bacterial suspension was added to each well to achieve a final concentration of approximately 1×10^6 CFU mL^{-1}. Bacterial suspensions without nanoparticles and wells containing particles and TSB without bacteria were used as controls. Using a microtiter plate reader (Biotek, ELx800), the minimal inhibitory concentration (MIC, the lowest concentration of an antimicrobial that will inhibit the visible growth of a microorganism after overnight incubation) values were determined by measuring the turbidity of the bacterial suspension after 24 h incubation at 37 °C. The effect of light scattering induced by the nanocapsules was taken into account when reading ABS_{600}. The results were confirmed visually. All assays were performed in triplicate.

3. Results and discussion

The general approach to synthesize potato starch nanocapsules with AgNPs embedded within their walls is shown in Fig. 1a. A macroemulsion is first prepared by mixing potato starch and silver nitrate in aqueous medium with an amphiphilic surfactant polyglycerin-polyricinoleate (PGPR) in cyclohexane. A miniemulsion is then generated by sonication of this mixture in order to achieve homogenous aqueous droplets in the cyclohexane phase. In a next step 2,4-toluene diisocyanate (TDI) is added in order to facilitate the formation of the core–shell structure of starch–AgNP nanocapsules *via* polyaddition. The nanocapsule shell is formed by cross-linking of the starch OH groups with the –NCO groups of TDI. The mixture is then transferred from cyclohexane to an aqueous medium using the non-ionic surfactant Lutensol AT50, and this surfactant facilitates the redispersion of oil soluble nanocapsules into the water phase. In this synthetic procedure the starch acts as a reducing agent for silver nitrate. Reduction of silver nitrate into metallic silver occurs during the polyaddition and cross-linking steps facilitated by the release of free radicals[35] and D-glucose from the amylose component of starch.[36,37] The nanocapsules were stable over several months in both the hydrophobic continuous phase (cyclohexane) and when redispersed in water (data not shown). The characteristic surface plasmon resonance (SPR) bands of AgNPs with the absorption maxima at around 412 nm are evidence for the presence of AgNPs in the nanocapsule solution (Fig. 2), and the inset in Fig. 2 shows the resultant solution of starch silver nanocapsules (grayish brown color) *versus* the starch only nanocapsules. The purple color of starch only nanocapsules is as a result of addition of sulforhodamine 101 (SR101) fluorescent dye (data not shown).

The proportion of non-volatile material contained in the miniemulsions left after the volatile solvent (water or cyclohexane) vaporized in the oven was calculated and expressed in the form of solid content (%) (Table 2). The loss in solid content of the redispersed sample is due to filtration of nanocapsules. The average sizes of the nanocapsules were determined by dynamic light scattering and are shown in Table 2. Formulations without addition of $AgNO_3$ (S046, S047 and S048) resulted in capsules in the size range of 700–800 nm.

SEM imaging further revealed that these nanocapsules are smaller in size but they were agglomerated and substantially deformed. A representative image of this type of nanocapsule is shown in Fig. 3d–f. When the synthesis was conducted in the presence of $AgNO_3$, a capsule size of 290–370 nm was achieved.

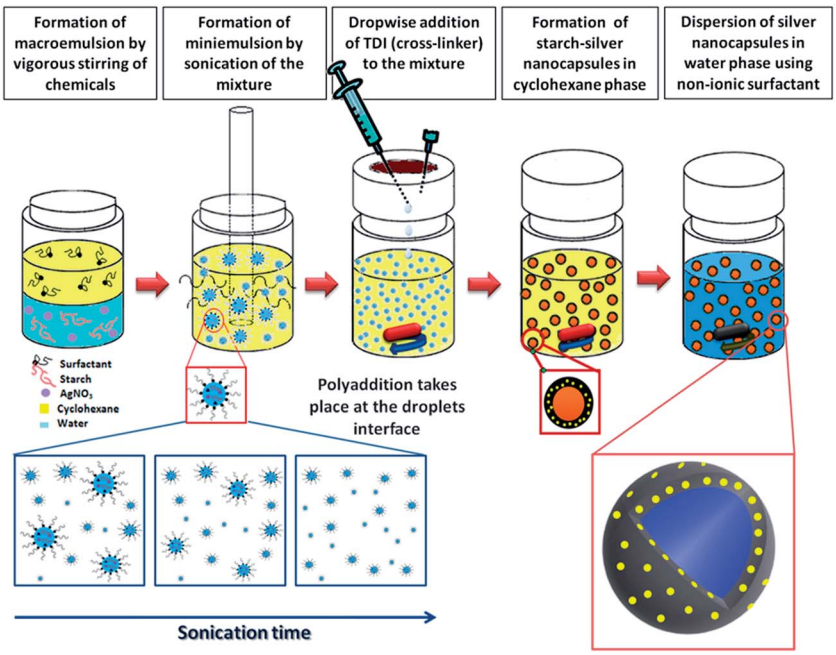

Fig. 1 Schematic of the procedure applied for synthesizing starch–AgNP nanocapsules.

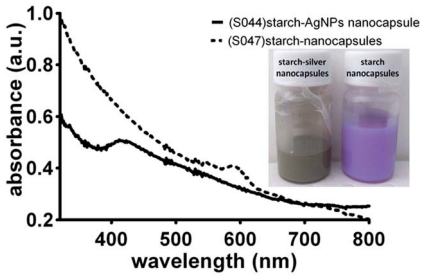

Fig. 2 UV-visible spectra of starch–silver nanocapsules *versus* starch only nanocapsules; the inset shows the appearance of the mini-emulsion solutions.

The SEM images of nanocapsules prepared with different amounts of TDI are shown in Fig. 3a–c. The images depict stable hollow spherical entities. Due to drying and vacuum required for SEM imaging the nanocapsules appear like hollow half balls. The images also show bright entities within the walls of the nanocapsules which are assigned to silver nanoparticles. The presence of metallic silver in the walls of the nanocapsules was also confirmed by energy-dispersive X-ray (EDX) spectroscopy which is discussed later in the paper (Fig. 5). It is interesting to note that the silver nanoparticles do not appear clear in the images of the nanocapsules presented in Fig. 3a. The reason for this is the greater shell wall thickness. These nanocapsules were synthesized using the highest amount of TDI. The dependence of the shell wall thickness on the concentration of TDI is discussed later in the paper. The SEM observations are an indication of the important role of $AgNO_3$ as an osmotic pressure agent.[38] Silver nitrate as an inorganic salt is insoluble in the oil phase and can act as a lipophobe that builds up an osmotic pressure in the droplets.[39] Thus, silver ions may be capable of suppressing Ostwald ripening and in this manner facilitate the formation of a well-defined core–shell structure. Analysis of the SEM images in Fig. 3a–c using the ImageJ software package

Table 2 Characteristics of nanocapsules: solid content, DLS size determination and carboxyl acid functionalities

		Solid content (%)		Mean diameter (nm)		Amount of –COOH groups on nanocapsules[a]		
Sample name	Chemistry of nano-capsules	C_6H_{12}	Redispersion[b]	C_6H_{12}	Redispersion	Groups per g (polymer)	Groups per particle	Groups per nm^2
S043	AgNP–starch nanocapsules	1.96	0.29	287.3	236.2	3.27×10^{18}	2.36×10^{4}	0.13
S044		1.71	0.44	373.8	147.1	4.09×10^{18}	7.13×10^{3}	0.10
S045		0.84	0.46	291.0	157.5	4.03×10^{18}	8.63×10^{3}	0.11
S046	Starch nanocapsules	0.50	0.37	815.8	527.9	3.05×10^{18}	2.46×10^{5}	0.28
S047		0.87	0.36	716.4	716.0	3.63×10^{18}	7.30×10^{5}	0.45
S048		1.14	0.41	807.5	445.7	4.05×10^{18}	1.96×10^{5}	0.31

[a] The amount of carboxylic groups was measured on redispersed samples. [b] Redispersion: dispersion of oil soluble nanocapsules in the water phase using Lutensol AT50.

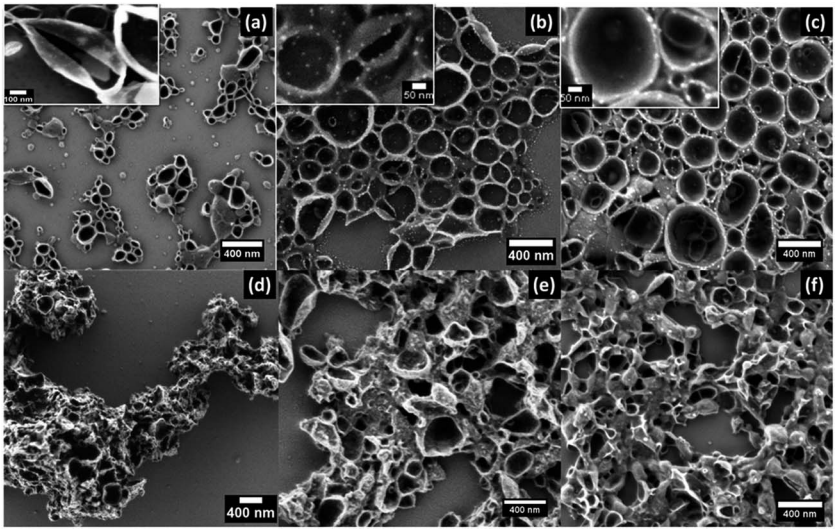

Fig. 3 SEM images of starch nanocapsules with and without silver nanoparticles: (a) S043, (b) S044, and (c) S045 which were synthesized with $AgNO_3$ and (d) S046, (e) S047, and (f) S048 which were synthesized without $AgNO_3$.

suggested round shaped silver nanoparticles of 14 nm diameter and a narrow size distribution. Furthermore, the size of the silver nanoparticles does not seem to be affected by the shell thickness. We calculated an average of 5.5 silver nanoparticles per each 100 nm^2 of the shell surface area. We hypothesize that the growth of nanoparticles is controlled during the formation of the nanocapsules' shell structure.

An SEM backscattered electron image of the silver nanoparticle containing nanocapsules is shown in Fig. 4a. Silver nanoparticles appear as bright points because of their capacity to scatter a larger number of electrons. EDX spectra recorded at positions 25 and 26 of the image presented in Fig. 4a are shown in Fig. 4b. Several peaks can be identified. These peaks are representative of the chemical composition of the nanocapsules. The peak at 3 keV is characteristic of the silver K and L lines and evidence for the presence of silver nanoparticles. The peak at 0.2 keV represents carbon. The peaks located at 0.38 and 0.5 keV are associated with the nitrogen and oxygen characteristic lines, respectively. The sodium line comes from the surfactants used in the formulation. There is a small Si line which is from the silicon wafer substrate used as a support. The distribution map of Ag is shown in Fig. 4c and shows a discrete and uniform distribution of silver in the nanocapsules.

The nanocapsule shell wall thickness was determined from the SEM images. Fig. 5 shows shell wall thicknesses as a function of the TDI amount used in the synthesis for formulations involving $AgNO_3$. It appears that the amount of added TDI significantly influences the nanocapsule shell thickness. As a general trend, the nanocapsule shell wall had a greater thickness with increasing TDI amount. For example, formulations S043, S044 and S045 where the TDI amount was 200, 150 and 100 mg had the shell thickness of 29 nm, 20 and 13 nm, respectively (Fig. 5).

Further insight into the distribution and size of the silver nanoparticles was revealed by TEM imaging. The TEM images in Fig. 6b demonstrate that a number of small 3–6 nm silver nanoparticles, which are beyond the resolution of SEM, are also available. On rare occasions we also observed the formation of some larger silver nanoparticles on a few tenths of nanometers as shown in the TEM image in Fig. 6a. The larger particles appear to have formed out of the nanocapsules and thus their growth has not been restricted by the walls.

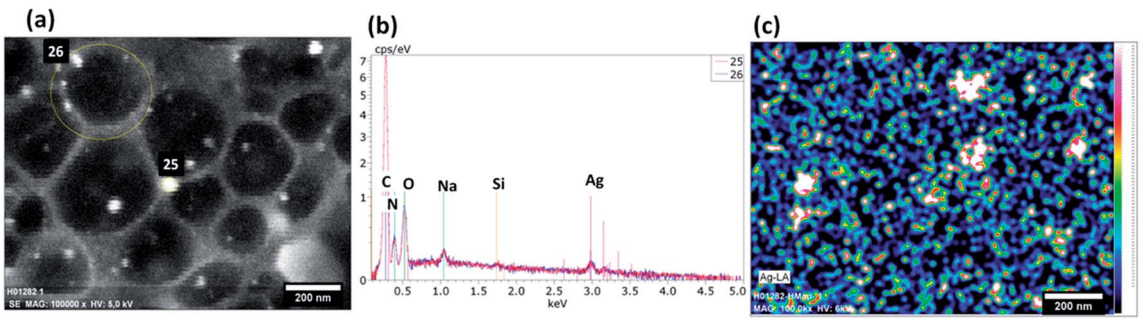

Fig. 4 (a) An SEM backscattered electron image; (b) EDX spectrum and (c) EDX image of the distribution of silver in the starch–silver nanocapsules.

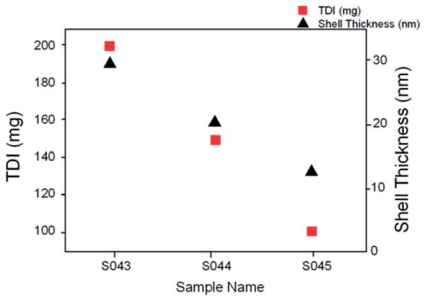

Fig. 5 Shell thickness *versus* the TDI amount used in the synthesis.

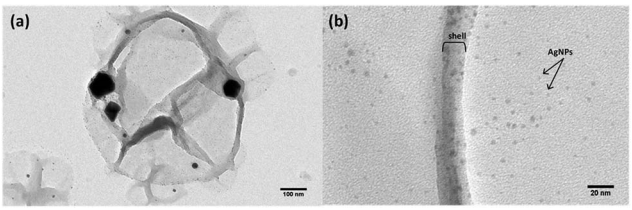

Fig. 6 TEM micrographs of a starch–silver nanocapsule (a) and a magnified image showing the capsule wall and smaller silver nanoparticles (b).

FTIR spectroscopy was applied to study the chemical composition of the samples (Fig. 7). The peak at 2276 cm^{-1} could be assigned to NCO groups; however, its low intensity suggests that in the final redispersed product most of these groups were consumed by the hydrolysis reaction with water to form amines.[40] A close examination of FTIR spectra suggests that the incorporation of silver nanoparticles does not lead to changes in the chemical composition of nanocapsules as in both compositions peaks identified with chemical bonds

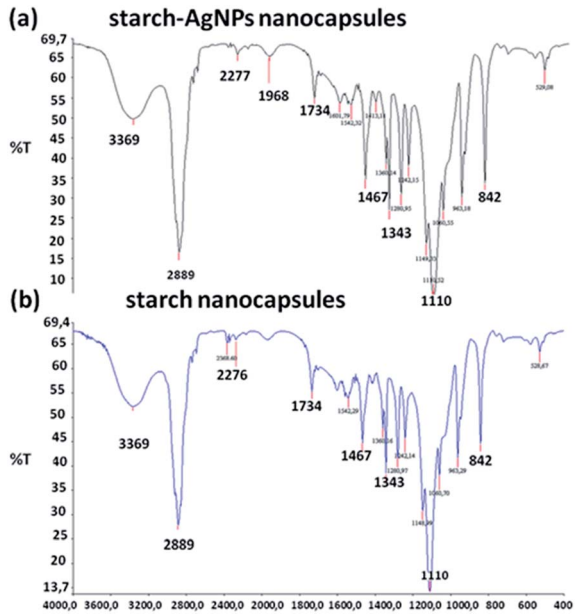

Fig. 7 FTIR spectra of the starch nanocapsules synthesized with (a) and without silver nitrate (b).

appear at the same frequencies. The presence of hydrogen bonded –OH stretching and NH valence vibration (which is overlapped by O–H vibration) is evident in the form of a broad band in the region of 3600–3200 cm^{-1}. A strong band at 2899 cm^{-1} is characteristic of the presence of CH (sp^3) stretching in the aromatic structure. The weak broad band at 1968 cm^{-1} is attributed to N–H/C–N groups. Free C=O vibration and polyurethane C=O vibration are observed at 1734 and 1700 cm^{-1}, respectively. The weak broad band at 1640 cm^{-1} is due to the formation of polyurea. The bands observed in the region of 1650–1450 cm^{-1} also indicate C=C vibration in the aromatic ring. C–O–C anti-symmetric bridge stretching is observed at 1150 cm^{-1} in the form of a medium intensity band (cm^{-1}). The bands at 1467 and 1343 cm^{-1} are attributed to CH_2 and CH bending respectively. The strong bands at 1300 and 1100 cm^{-1} are assigned to the C–(C=O)–C bending and C–O valence vibration. A strong band at 1060 cm^{-1} mainly originates from the tertiary alcohol (R–C(CH_3)–OH). The bands at 963, 842, 717 and 529 cm^{-1} are also attributed to the skeletal vibrations of the polymeric shell.

The outer shell wall of the nanocapsules was further functionalized by carboxymethylation[41] in order to provide appropriate chemical functionalities which could be used for chemical immobilization on surfaces[42] when targeted applications are antibacterial coatings or/and the attachment of proteins or other ligands.[40,43–45] The amount of carboxylic groups on the nanocapsule surface was determined by polyelectrolyte titration and the results are presented in Table 2. The average COOH functionalities in the samples containing AgNPs are in the range of 0.1–0.13 group per nm^2 and in pure starch nanocapsules they are between 0.28 and 0.45 group per nm^2. Such functional group densities are believed to be sufficient for immobilization purposes and also provide a sufficient number of binding sites for attachment of ligands or proteins.

The concentration of silver based on ICP analysis was 37 μg mL^{-1}. The decrease in the silver concentration compared to the initial amount used in the synthesis can be attributed to removal of silver nanoparticles which were not embedded in nanocapsule walls during the washing and centrifuge steps.

Finally, we examined the MIC of the nanocapsules against *Staphylococcus epidermidis* (*S. epidermidis*) and *Escherichia coli* (*E. coli*). These two bacteria pose a significant medical problem and cause a substantial part of the infections. The concentration of bacteria used for determination of the MIC values was 1×10^6 CFU mL^{-1}. The minimum concentration of starch–silver nanocapsules required for inhibition of bacteria growth was studied by serial dilution. We found that a very low concentration of starch–silver nanocapsules was able to

Table 3 MIC of starch–silver nanocapsules (S043) against *Staphylococcus epidermidis* ATCC 35984 and *Escherichia coli* ATCC 25922

Bacteria	MIC (μg mL^{-1})
S. epidermidis ATCC 35984	2.315[a]
E. coli ATCC 25922	2.315[a]

[a] The mean values are shown with STD: <0.5.

inhibit the bacteria growth. These concentrations are shown in Table 3 and were 2.315 μg mL^{-1} for both *S. epidermidis* and *E. coli*. The growth was completely inhibited at 2.315 μg mL^{-1} in starch–silver nanocapsules while starch nanocapsules without silver nanoparticles had no inhibitory effect on bacterial growth.

Generation of hybrid polymeric/metallic nanocapsules in a controllable manner is a challenging task.[22,46–48] In this work, we were able to employ the miniemulsion technique in combination with polyaddition polymerization to prepare in a controllable manner silver nanoparticles that are incorporated in the walls of potato starch nanocapsules. These nanocapsules have strong antibacterial properties with MICs in the range of a few micrograms per milliliter for *S. epidermidis* (Gram-positive) and *E. coli* (Gram-negative). This type of antibacterial nanocapsule could be of interest in biomedical applications because they might be capable of reducing the rates of infections when such carriers are used in drug delivery. The material is also interesting because starch is biodegradable, which means that it would be broken down by natural physiological processes if delivered into the body. Current work in our lab is focused on immobilization of these starch–silver nanocapsules to solid surfaces for applications as antibacterial coatings that can be applied to wound dressing and implantable biomedical devices. We are also exploring loading of various therapeutic agents in these hybrid nanocapsules that can be delivered either *via* solid carriers or in a suspension form.

4. Conclusion

In summary, we report a facile method for synthesis of hollow starch nanocapsules decorated with silver nanoparticles. The addition of $AgNO_3$ seems to play an important role facilitating the formation of stable spherical nanocapsules. The nanocapsule wall thickness can be controlled by the amount of TDI used in the synthesis. We were able to conduct further surface modification of the nanocapsule walls in order to provide carboxyl functional groups which can be potentially used for the surface immobilization or binding of ligands of interest for a particular application. The silver nanoparticles were formed in capsule walls and had diameters of about 14 nm. However, TEM images revealed the presence of some quantity of smaller particles. Occasionally, large nanoparticles of a few tenths of nanometers were also observed but they appear to have grown outside of capsule walls. MIC studies showed high antibacterial efficacy against *Staphylococcus epidermidis* ATCC 35984 and *Escherichia coli* ATCC 25922. The biocompatible nanostructures presented in this paper are of potential interest for various biomedical applications such as smart drug carriers and antibacterial coatings for medical devices and wound dressings.

Acknowledgements

The authors would like to thank the staff and students of Max-Planck Institute for Polymer Research for their kind support. University of South Australia (UniSA) and Australian Nanotechnology Network (ANN) are acknowledged for financial support. KV thanks the ARC for fellowship no. FT100100292.

References

1 P. W. Stone, *Expert Rev. Pharmacoecon. Outcomes Res.*, 2009, **9**, 417–422.
2 L. Paitoonpong, C. K. B. Wong and T. M. Perl, *Infect. Dis. Epidemiol.*, 2013, 369.
3 K. Ho, *Perspect. Biol. Med.*, 2001, **44**, 1–16.
4 M. L. Cohen, *Science*, 1992, **257**, 1050–1055.
5 N. Høiby, T. Bjarnsholt, M. Givskov, S. Molin and O. Ciofu, *Int. J. Antimicrob. Agents*, 2010, **35**, 322–332.
6 H. Klasen, *Burns*, 2000, **26**, 117–130.
7 H. Klasen, *Burns*, 2000, **26**, 131–138.
8 Y.-S. KIM and J.-Y. KIM, *WO Pat.*, 2,007,105,883, 2007.
9 J. Wu, Y. Zheng, W. Song, J. Luan, X. Wen, Z. Wu, X. Chen, Q. Wang and S. Guo, *Carbohydr. Polym.*, 2013, **102**, 762–771.
10 S. Meenakumari, K. D. Arunachalam and A. S. Kumar, *Asian J. Chem.*, 2013, **25**, S347–S349.
11 D. Roe, B. Karandikar, N. Bonn-Savage, B. Gibbins and J.-B. Roullet, *J. Antimicrob. Chemother.*, 2008, **61**, 869–876.
12 C. Marambio-Jones and E. M. Hoek, *J. Nanopart. Res.*, 2010, **12**, 1531–1551.
13 M. K. Rai, S. D. Deshmukh, A. P. Ingle and A. K. Gade, *J. Appl. Microbiol.*, 2012, **112**, 841–852.
14 K. Vasilev, J. Cook and H. J. Griesser, *Expert Rev. Med. Devices*, 2009, **6**, 553–567.
15 J. S. Kim, E. Kuk, K. N. Yu, J.-H. Kim, S. J. Park, H. J. Lee, S. H. Kim, Y. K. Park, Y. H. Park and C.-Y. Hwang, *Nanomedicine*, 2007, **3**, 95–101.
16 O. Choi, K. K. Deng, N.-J. Kim, L. Ross Jr, R. Y. Surampalli and Z. Hu, *Water Res.*, 2008, **42**, 3066–3074.
17 S. Prabhu and E. K. Poulose, *Int. Nano Lett.*, 2012, **2**, 1–10.
18 S. Chernousova and M. Epple, *Angew. Chem., Int. Ed.*, 2013, **52**, 1636–1653.
19 K. Mijnendonckx, N. Leys, J. Mahillon, S. Silver and R. Van Houdt, *BioMetals*, 2013, 1–13.
20 K. A. Eid and H. M. Azzazy, *Nanomedicine*, 2013, 1–8.
21 K. Morrill, K. May, D. Leek, N. Langland, L. D. Jeane, J. Ventura, C. Skubisz, S. Scherer, E. Lopez and E. Crocker, *J. Altern. Complement. Med.*, 2013, **19**, 224–231.
22 K. Landfester and V. Mailänder, *Expert Opin. Drug Delivery*, 2013, **10**, 593–609.
23 J. Sudimack and R. J. Lee, *Adv. Drug Delivery Rev.*, 2000, **41**, 147–162.
24 G. Baier, D. Baumann, J. M. Siebert, A. Musyanovych, V. Mailänder and K. Landfester, *Biomacromolecules*, 2012, **13**, 2704–2715.
25 B. Blaiszik, N. Sottos and S. White, *Compos. Sci. Technol.*, 2008, **68**, 978–986.
26 D. Y. Wu, S. Meure and D. Solomon, *Prog. Polym. Sci.*, 2008, **33**, 479–522.
27 J. Fickert, M. Makowski, M. Kappl, K. Landfester and D. Crespy, *Macromolecules*, 2012, **45**, 6324–6332.
28 C. Yongping, T. Jabbour and L. Xingde, in *Lasers and Electro-Optics (CLEO), 2011 Conference on*, 2011, pp. 1–2.

29 K. Landfester, *Angew. Chem., Int. Ed.*, 2009, **48**, 4488–4507.
30 J. Devy, E. Balasse, H. Kaplan, C. Madoulet and M. C. Andry, *Int. J. Pharm.*, 2006, **307**, 194–200.
31 A. Bajpai and S. Bhanu, *J. Mater. Sci. Mater. Med.*, 2007, **18**, 1613–1621.
32 M. C. Lévy and M. C. Andry, *Int. J. Pharm.*, 1990, **62**, 27–35.
33 A. Musyanovych, R. Rossmanith, C. Tontsch and K. Landfester, *Langmuir*, 2007, **23**, 5367–5376.
34 J. M. Andrews, *J. Antimicrob. Chemother.*, 2001, **48**, 5–16.
35 D. Crespy and K. Landfester, *Beilstein J. Org. Chem.*, 2010, **6**, 1132.
36 P. Raveendran, J. Fu and S. L. Wallen, *J. Am. Chem. Soc.*, 2003, **125**, 13940–13941.
37 N. Vigneshwaran, R. P. Nachane, R. H. Balasubramanya and P. V. Varadarajan, *Carbohydr. Res.*, 2006, **341**, 2012–2018.
38 K. Landfester, M. Willert and M. Antonietti, *Macromolecules*, 2000, **33**, 2370–2376.
39 K. Landfester, *Annu. Rev. Mater. Res.*, 2006, **36**, 231–279.
40 G. Baier, A. Musyanovych, M. Dass, S. Theisinger and K. Landfester, *Biomacromolecules*, 2010, **11**, 960–968.
41 U. Paiphansiri, J. Dausend, A. Musyanovych, V. Mailänder and K. Landfester, *Macromol. Biosci.*, 2009, **9**, 575–584.
42 R. V. Goreham, A. Mierczynska, M. Pierce, R. D. Short, S. Taheri, A. Bachhuka, A. Cavallaro, L. Smith and K. Vasilev, *Thin Solid Films*, 2013, **528**, 106–110.
43 E. Kim, D. Kim, H. Jung, J. Lee, S. Paul, N. Selvapalam, Y. Yang, N. Lim, C. G. Park and K. Kim, *Angew. Chem.*, 2010, **122**, 4507–4510.
44 C. E. Mora-Huertas, H. Fessi and A. Elaissari, *Int. J. Pharm.*, 2010, **385**, 113–142.
45 Y. Chen, H. Chen, D. Zeng, Y. Tian, F. Chen, J. Feng and J. Shi, *ACS Nano*, 2010, **4**, 6001–6013.
46 A. Ethirajan and K. Landfester, *Chem. – Eur. J.*, 2010, **16**, 9398–9412.
47 J.-T. Zhang, G. Wei, T. F. Keller, H. Gallagher, C. Stötzel, F. A. Müller, M. Gottschaldt, U. S. Schubert and K. D. Jandt, *Macromol. Mater. Eng.*, 2010, **295**, 1049–1057.
48 M. Tan, G. Chow, L. Ren and Q. Zhang, in *NanoScience in Biomedicine*, ed. D. Shi, Springer, Berlin Heidelberg, 2009, pp. 272–289.